Optics Communications 333 (2014) 265–273

Contents lists available at ScienceDirect

Optics Communications

journal homepage: www.elsevier.com/locate/optcom

Influence of space–time speckle effect on the image quality in a synthetic aperture imaging ladar

Qian Xu, Yu Zhou*, Jianfeng Sun, Zhiwei Sun, Xiaoping Ma, Liren Liu

Key Laboratory of Space Laser Communication and Detection Technology, Shanghai Institute of Optics and Fine Mechanics, Chinese Academy of Sciences, No. 390, Qinghe Road, Jiading District, Shanghai 201800, People's Republic of China

ARTICLE INFO

Article history:
Received 25 February 2014
Received in revised form
9 July 2014
Accepted 10 July 2014
Available online 23 July 2014

Keywords:
Speckle
Synthetic aperture radar
Lidar
Image quality

ABSTRACT

Temporally and spatially varying speckle effect arises as a consequence of the frequency modulation chirped laser signal employed in synthetic aperture imaging ladar (SAIL).A variety of reconstructed images degraded by laser speckle effect have been reported. In this paper, space–time speckle effects and their influence on imaging based on the SAIL system in a far-field diffraction region are systematically studied. The first half of this paper provides the theoretical analyses of the 2D data acquisition with speckle effect in SAIL. Numerical simulations of the temporally varying speckle pattern, the integrated speckle field over a receiving antenna and their influence to the image quality for SAIL are obtained in the remaining of the paper. Our results will be valuable for further studies on the suppression of speckle effect in SAILs.

1. Introduction

Synthetic aperture imaging ladar (SAIL), which applies synthetic aperture radar (SAR) techniques in the optical laser radar domain, can theoretically provide centimeter-class resolution with a small-diameter optical aperture in 1000 km [1]. As a ladar platform moves, a sequence of closely spaced pulses is repeatedly transmitted on a slant target plane and the echoes are correspondingly recorded. The returned signals are heterodyne detected with a local oscillator (LO) signal, and then processed with deramp compression in the orthogonal direction of travel (range direction) and with a matched filtering imaging algorithm in the travel direction (azimuth direction).

Given that a frequency modulation (FM) chirped laser signal is always employed as the transmitting signal, SAIL is inevitably influenced by speckle effect. A speckle pattern, which has a distinctive granular appearance, is formed when a laser beam is reflected from the rough surface of a target plane [2]. Previous studies have shown the impact of SAIL speckle effect on signal-to-noise ratio (SNR) in photon-limited heterodyne detection [3,4]. The statistical characteristics of space–time speckle effect have also been obtained from the theory of partially coherent light and a complex coherence function of integrated speckle over antenna aperture has been defined [5,6]. However, speckle effect not only decreases the SNR in heterodyne detection but also reduces imaging quality. A variety of SAIL 2D reconstructed images reported by several institutes are degraded by laser speckle effect [7–9].

Our research demonstrates both temporally and spatially varying speckle effects and their influence on SAIL image quality. Based on the SAIL system in a far-field diffraction region, the physical model of speckle effect in SAIL is established, and the optical field of complex amplitude for the speckle pattern on the receiving plane is obtained. Temporally and spatially varying speckle effects are analyzed based on the wavelength linear chirped signal. Furthermore, 2D data acquisition of SAIL and image reconstruction with speckle effect are theoretically deduced. The temporally varying speckle pattern and the integrated speckle field over a receiving antenna, as well as their influence on the SAIL image quality are numerically obtained.

In Section 2, the acquisition of 2D imaging data for a resolution element of SAIL and the corresponding image reconstruction are reviewed. Physical models of temporally and spatially varying speckle effect are established and the shift of the speckle pattern within the scope of the receiving antenna is analyzed. Subsequently, the integrated speckle field over a receiving antenna aperture and the 2D data collection equation of SAIL with speckle effect are deduced. Analyses are then generalized to the area distributive target. Section 3 presents the numerical simulation results of the temporally varying speckle pattern and the integrated speckle field over a receiving antenna, as well as their influence to the image quality for SAIL. Conclusions are provided in Section 4.

* Corresponding author.
E-mail address: sunny@mail.siom.ac.cn (Y. Zhou).

http://dx.doi.org/10.1016/j.optcom.2014.07.034

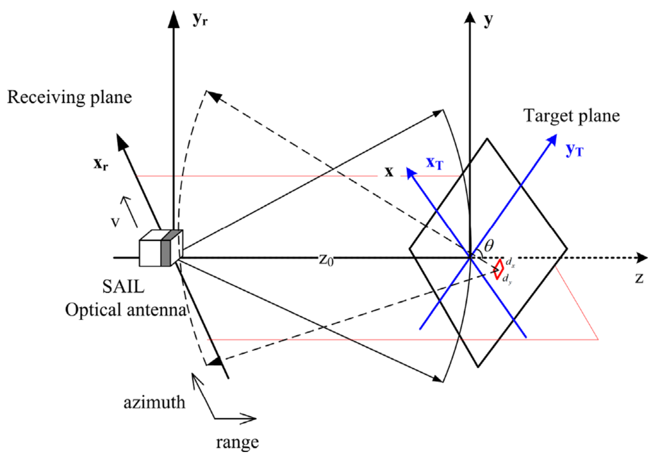

Fig. 1. The strip-mode SAIL geometry.

2. Data acquisition with speckle effect in SAIL

Fig. 1 illustrates the strip-mode SAIL geometry. The coordinate system of the SAIL transmitting antenna is (x_r, y_r), and the target coordinate system is (x_T, y_T), which is inclined at θ with respect to the beam. The x axis represents the azimuth direction and the range between SAIL and the center of the target plane is z_0. Given that a rectangular aperture provides a better imaging resolution than a circular aperture [10], the telescope of the transmitting antenna has been assumed to have a rectangular aperture of $L_x L_y$, whereas the optical aperture of the receiving telescope is $D_x D_y$. For simplicity, we assume $L_x D_x$ and $L_y D_y$ in this study.

2.1. 2D data acquisition and image formation

In SAIL, the optical antenna moves with a constant velocity v while illuminating the target plane and repeatedly transmiting the FM chirped laser pulses. Fast time along the range direction is defined as $t_f (0 \le t_f \le T_f).T_s$ is the interval between the transmitted pluses, and the discrete slow time t_s is equal to nT_s in the azimuth direction. The average wavelength is λ. An arbitrary resolution element with a scale of $d_x \times d_y$ and coordinates (x_T, y_T) on the target plane has the coordinate transfer as [6]

$$x = x_T, \quad y = y_T \sin\theta, \quad z = z_0 + y_T \cos\theta \tag{1}$$

With a temporal phase signal, the optical field of the telescope transmitting antenna can be described by

$$E_1(x_r, y_r, t_{nf}) = A_1 \mathrm{rect}\left(\frac{x_r}{L_x}\right)\mathrm{rect}\left(\frac{y_r}{L_y}\right)\exp\left\{j2\pi\left[f_0 t_{nf} + \dot{f}\frac{t_{nf}^2}{2}\right]\right\} \tag{2}$$

where f_0 is the starting frequency, $\dot{f}$ is the chirp rate of the FM chirp signal, and t_{nf} is the fast time at the nth pulse. The diffracted field of the point (x_T, y_T) on the target plane can be written as

$$E_2(x_T - nvT_s, y_T) = A_1 \frac{L_x L_y}{j\lambda z} \sin c\left(\frac{(x_T - nvT_s)L_x}{\lambda z}\right) \sin c\left(\frac{y_T L_y}{\lambda z}\right) \times \exp\left(j\frac{2\pi z}{\lambda}\right)\exp\left[j\pi\frac{(x_T - nvT_s)^2 + (y_T \sin\theta)^2}{\lambda z}\right] \tag{3}$$

At the receiving plane, the return field backscattered from the resolution element can be obtained by

$$\begin{aligned} E_3(x_r, y_r, x_T, y_T : t_{nf}, nT_s) &= E_2(x_T - nvT_s, y_T)\rho(x_T - nvT_s, y_T)\exp[j\varphi(x_T - nvT_s, y_T)] \\ &\times \sin c\left(\frac{(x_T - nvT_s - x_r)d_x}{\lambda z}\right) \sin c\left(\frac{(y_T - y_r)d_y}{\lambda z}\right) \\ &\times \frac{d_x d_y}{j\lambda z}\exp\left(j\frac{2\pi}{\lambda}z\right)\exp\left[j\pi\frac{(x_T - nvT_s - x_r)^2 + (y_T - y_r)^2}{\lambda z}\right] \\ &\times \exp\left\{j\pi\left[f_0(t_{nf} - \tau) + \dot{f}\frac{(t_{nf} - \tau)^2}{2}\right]\right\} \end{aligned} \tag{4}$$

where $\rho(x_T - nvT_s, y_T)$ is the reflectivity of the Lambertian target, $\varphi(x_T - nvT_s, y_T)$ is the reflective phase that depends on surface properties, and $\tau = 2z/c$ is the round-trip delay time. When heterodyne is received by the optical antenna and the detector, the beat frequency photocurrent can be deduced by

$$\begin{aligned} I_{1D}(x_T, y_T; t_{nf}, nT_s) &= \eta A_1{}^2 \frac{L_x L_y}{j\lambda z}\frac{d_x d_y}{j\lambda z}\rho(x_T - nvT_s, y_T)\exp[j\varphi(x_T - nvT_s, y_T)] \\ &\times \sin c^2\left(\frac{(x_T - nvT_s)L_x}{\lambda z}\right) \sin c^2\left(\frac{y_T L_y}{\lambda z}\right) \\ &\times \sin c\left(\frac{(x_T - nvT_s - x_r)d_x}{\lambda z}\right) \sin c\left(\frac{(y_T - y_r)d_y}{\lambda z}\right) rect\left(\frac{t_{nf} - T_f/2}{T_f}\right) \\ &\times \exp\left(j2\pi\frac{{y_T}^2}{\lambda z}\right) \times \exp\left(j2\pi\dot{f}t_{nf}\frac{2\Delta z_T}{c}\right)\exp\left[j2\pi\frac{(x_T - nvT_s)^2}{\lambda z}\right] \end{aligned} \tag{5}$$

$\Delta z_T = z - L_{loc}/2$, where L_{loc} is the round-trip delay of the LO. The SAIL 2D data collection equation for an individual resolution element $d_x \times d_y$ has the form

$$I_{2D}(x_T, y_T; t_f, t_s) = \sum_n I_{1D}(x_T, y_T; t_{nf}, nT_s) \tag{6}$$

Notice that the footprint D_{fp} can be defined as the common area of the illuminated area and the detectable areas on target plane [6]. Thus the optical footprint function is given by

$$D_{fp}(x, y) = \sin c^2\left(\frac{(x_T - nvT_s)L_x}{\lambda z}\right) \sin c^2\left(\frac{y_T L_y}{\lambda z}\right) \tag{7}$$

Therefore, the full width at minimum of the optical footprint size is$D_{fp}^x \times D_{fp}^y = 2\lambda z/L_x \times 2\lambda z/L_y$.

Regarding the SAIL image reconstruction [6], the resolution function in the range direction can be obtained by the Fourier transform

$$I_R(y) = \sin c\left(\frac{2\dot{f}t_{nf}}{c}\Delta z_T\right) \tag{8}$$

For simplicity, factors unrelated to fast time are ignored. Furthermore, the azimuth resolution is acquired by using a matched filtering algorithm, and the conjugated quadratic phase is given by$\exp\left[-j\frac{2\pi}{\lambda z}(vnT_s)^2\right]$. The azimuth imaging resolution can then be written as

$$\begin{aligned} I_A(x) &= \exp\left[j2\pi\frac{x_T^2 - (vnT_s)^2}{\lambda z}\right] D_{fp}^x \sin c\left[\frac{(x_T - vnT_s)D_{fp}^x}{\lambda z}\right] \\ &* \left(\frac{\lambda z}{L_x}\right)^2 tri\left[\frac{(x_T - nvT_s)}{L_x/2}\right] \end{aligned} \tag{9}$$

2.2. Space–time speckle effect

Fig. 2 illustrates the formation of speckle in SAIL. Speckle patterns, with the peculiar granular appearance and random phase distribution, are formed when the transmitted optical field is reflected from a diffused target surface. In this section, speckle effect is characterized through a resolution element of the target [11]. The speckle characteristics of the area distributive target composed of multiple resolution elements are further studied in Section 2.4.

As depicted in Fig. 3, the resolution element is divided into $N \times N$ pixels with a sampling interval of $\delta x \times \delta y$, thereby conforming to the